

Flavia G. Durán
Bibiana P. Barbero
Luis E. Cadús

Instituto de Investigaciones en
Tecnología Química (INTEQUI),
UNSL – CONICET, San Luis,
Argentina.

Research Article

Catalytic Combustion of Ethyl Acetate over Manganese Oxides Deposited on Metallic Monoliths

MnO_x/AISI 304 austenitic stainless-steel monolithic catalysts were prepared by impregnation with aqueous solutions of manganese nitrate or acetate. The preparation method was satisfactory in terms of reproducibility and adherence of the deposited phase. The use of different precursors led to significantly dissimilar results. With manganese nitrate, the formation of Mn-Cr-O mixed phases on the surface was favored, whereas with manganese acetate, Mn₂O₃ was the predominant active phase. The Mn-Cr-O mixed phases would be highly dispersed but their catalytic activity was low. The major catalytic behavior was obtained with monoliths impregnated with manganese acetate.

Keywords: Catalysis, Catalytic combustion, Coatings, Pollutants

Received: June 10, 2013; *revised:* October 11, 2013; *accepted:* November 19, 2013

DOI: 10.1002/ceat.201300389

1 Introduction

Many industrial activities generate gaseous emissions containing volatile organic compounds (VOCs) which are an important source of atmospheric pollution. In order to turn them into an environmentally sustainable process, it is necessary to avoid such emissions. This can be efficiently achieved by means of catalytic combustion [1].

The application of this technology requires the deposition of the catalytically active phase on the walls of a structured support, such as the well-known monoliths [2]. Traditionally, monoliths were made of cordierite, a ceramic material with low thermal expansion coefficient and an adequate porosity to act as catalytic support. In the last years, metallic monoliths have become an interesting alternative to the classic ceramic ones, due to their higher thermal conductivity, greater mechanical shock resistance, and the possibility of thinner walls allowing low pressure drop with high cell density [2]. The difficulty for the use of a metallic support is the low specific surface area and the low roughness which causes bad adhesion of the active phase to the metallic surface. In order to overcome this problem, a suitable treatment for the metallic surface is required. In pure aluminum monoliths, anodization produces a well-adhered porous alumina layer on the surface [3]. In the case of Al-alloyed ferritic stainless-steel monoliths, a thermal

treatment at high temperature (900 °C for 22 h) provokes the migration of the aluminum to the surface, generating an alumina layer in form of whiskers that allows anchoring of the wash-coating [2, 4, 5]. For applications at moderate temperatures (below 750 °C), such as the catalytic combustion of VOCs, austenitic stainless steels are an interesting alternative to the application of ferritic alloys containing Al. Austenitic stainless steels are cheaper and under oxidizing conditions at high temperature they generate a scale of metal transition oxides containing Cr, Fe, and Mn [6, 7].

In a previous work [8], a study was performed on the determination of the optimal thermal treatment conditions for obtaining an oxide scale with adequate characteristics to further deposition of the catalytic phase on AISI 304 austenitic stainless steel. After evaluating several temperatures and times of treatment as well as the fluid dynamics of the treatment atmosphere, a homogeneous and well-adhered oxide scale was obtained at 900 °C for 2 h in synthetic air flow. In fact, no mass loss was detected during the adherence test in an ultrasound bath. According to the XRD results, the scale is formed by Cr₂O₃ and Mn_{1+x}Cr_{2-x}O_{4-x}. Considering that these phases could present catalytic activity [9–11], the monolith was evaluated in ethyl acetate combustion, and indeed, activity was observed at reaction temperatures above 250 °C, achieving total conversion of ethyl acetate at around 420 °C. Although this result is not negligible, it is known that monolithic catalysts with a higher activity in reactions of VOC combustion are possible [4, 12]. Therefore, the aim of this work is to increase the catalytic activity of metallic monoliths built in AISI 304 austenitic stainless steel by means of the deposition of manganese oxide, which is widely recognized as an excellent catalyst in combustion reactions [12, 13].

Correspondence: Dr. Flavia G. Durán (fduran@unsl.edu.ar), Instituto de Investigaciones en Tecnología Química (INTEQUI), UNSL – CONICET, Chacabuco 917, D5700BWS San Luis, Argentina.

The thermal treatment of AISI 304 stainless steel generates a rough oxide scale on the surface [8]. It is, in principle, very adequate for depositing an active phase by means of the traditional wash-coating method from a suspension of fine catalyst particles. This procedure requires the previous synthesis of the powdered catalyst, preparation of a stable suspension, and well-controlled deposition stages (immersion time, withdrawn rate, drying and calcination conditions, etc.). With the aim to simplify the deposition of the active phase, an impregnation method from aqueous solutions of precursor salts is proposed. This kind of preparation avoids the steps of powder catalyst synthesis and suspension preparation. However, it is worth taking into account that, depending on the precursor, the physical chemistry of the active phase would differ. Hence, in this work, two possible precursors for manganese oxide were tested: manganese nitrate and manganese acetate. Both salts are perfectly soluble in water, thus avoiding problems in preparing the solutions. Besides, the most interesting fact is that the manganese nitrate solution contains Mn^{2+} ions in acid medium while the manganese acetate generates manganese(II) acetate complexes in solution. Consequently, the interaction of manganese with the components of the oxide scale on the surface of the stainless steel would be significantly different in each case.

2 Experimental

2.1 Preparation of the Monolithic Catalysts

The bare monoliths were prepared as described elsewhere [8]. Briefly, AISI 304 austenitic stainless-steel sheets (Cr 19%, Ni 9.2%, Mn 2%, C < 0.08%, and Fe balance) with 0.05 mm thickness were employed. Each monolith was formed by rolling around a spindle alternate flat and corrugated sheet resulting in a cylinder of 30 mm height, 16 mm diameter, and a cell density of 60 cells per cm^2 . Then, the monoliths were thermally treated under flow of synthetic air at 900 °C for 2 h and cooled down to room temperature under the same atmosphere. The monoliths obtained were denoted as bare monoliths (BM).

For impregnation, an aqueous solution of $Mn(CH_3COO)_2 \cdot 4H_2O$ (Anhedra) (2.6 M and pH 6) or an aqueous solution of $Mn(NO_3)_2 \cdot 4H_2O$ (Fluka) (10 M and pH 2) was used. Each solution was prepared at 50% of the saturation concentration, with the following objectives: (i) to assure a total dissolution of salts, and (ii) to obtain solutions sufficiently concentrated in order to minimize the immersion numbers leading to an adequate amount of active phase. Due to a higher solubility of manganese nitrate, its solution became more concentrated than the manganese acetate solution, but this did not hinder the evaluation of the different manganese precursors. In both cases, the bare monoliths were immersed in the solution and agitated by orbital stirring for 1 h. After that, the monoliths were withdrawn and the excess of solution was removed by blowing air at 6 psig during 40 s in order to avoid obstruction of monolith channels. To increase the amount of catalyst loaded on the monoliths, three immersions were performed and after each, the impregnated monoliths were dried at 80 °C during 24 h and calcined at 500 °C for 3 h. The monolithic cat-

alysts were named xMn-p, where x is the number of impregnations and p is the precursor: manganese acetate (a) or manganese nitrate (n).

2.2 Characterization

2.2.1 Adherence Test

The adherence of the coating was evaluated in terms of the weight loss after submitting the monoliths to ultrasonic vibration. The coated monoliths were immersed in 25 mL petroleum ether inside a sealed beaker and then treated in an ultrasound bath for 30 min. After ultrasonic treatment, the sample was dried at 120 °C for 1 h. Under these conditions, the mass of solvent that remained in the sample was not significant. The weight loss was presented as percentage of the total coating.

2.2.2 X-Ray Diffraction (XRD)

XRD patterns were obtained by using a Rigaku diffractometer operated at 30 kV and 25 mA by employing V-filtered Cr $K\alpha$ radiation ($\lambda = 0.2291$ nm) in continuous scan mode from 30° to 140° of 2θ using 0.05° sampling interval. The crystalline phases were identified by reference to powder diffraction data. The XRD characterization was performed on a sheet of stainless steel used as reference. This sheet of stainless steel was thermally treated together with the monoliths and it was impregnated under the same conditions of the monoliths.

2.2.3 BET Surface Area Measurements (S_{BET})

The surface area was measured by means of the BET method from N_2 adsorption isotherm at liquid nitrogen temperature in a Micromeritics Gemini V apparatus with a homemade cell for analyzing the whole monoliths.

2.2.4 X-Ray Photoelectron Spectroscopy (XPS)

The XPS analyses were performed in a multi-technique system (SPECS) equipped with an Al-monochromatic X-ray source, and a hemispherical PHOIBOS 150 analyzer operating in the fixed analyzer transmission (FAT) mode. The spectra were obtained using a monochromatic Al $K\alpha$ X-ray source ($h\nu = 1486.6$ eV) operated at 150 W. The pass energy for the element scan was 30 eV. The working pressure in the analyzing chamber was less than 2×10^{-8} mbar. The data treatment was performed with the Casa XPS program (Casa Software Ltd, UK). The peak areas were determined by integration, employing a Shirley-type background. Peaks were considered to be a mixture of Gaussian and Lorentzian functions. For quantification of the elements, sensitivity factors provided by the manufacturer were used.

2.3 Catalytic Test

The monoliths were evaluated in the combustion of ethyl acetate. The reacting stream was $300 \text{ cm}^3 \text{ min}^{-1}$ containing $4000 \text{ mg C per m}^3$ diluted in synthetic air. The space velocity was 3750 h^{-1} . The gaseous mixture was analyzed before and after reaction by gas chromatography using a Buck Scientific Mod 910 equipped with an FID detector, a methanizer, and a Carbowax 20M/Chromosorb W column. Reported data were the average of at least two results in stationary state.

3 Results

3.1 Weight Gain and Adherence of the Active Phase

The percentages of weight gain of each monolith are presented in Fig. 1. The average values are summarized in Tab. 1. As it can be observed, with both precursors the retained mass linearly increased with the impregnation numbers. The weight gain of monoliths impregnated with manganese nitrate was notably higher than that of monoliths impregnated with manganese acetate.

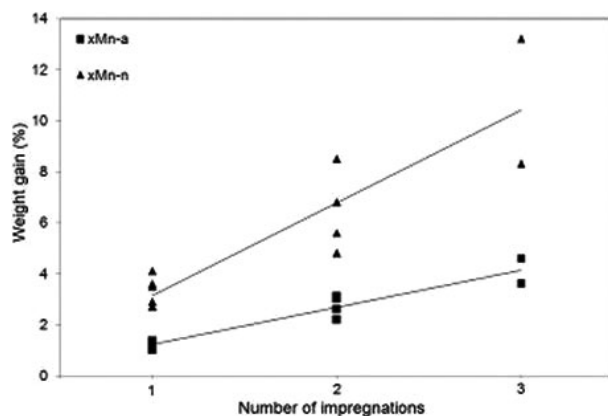


Figure 1. Percentage of weight gain as a function of the impregnation number.

Table 1. Weight gain after impregnation, weight loss during the adherence test, surface area per monolith, and $\text{Mn}_{2p3/2}/\text{Cr}_{2p}$ atomic ratio from XPS.

Monolithic catalyst	Weight gain [%]	Weight loss [%]	S_{BET} [$\text{m}^2 \text{ monolith}^{-1}$]	$\text{Mn}_{2p3/2}/\text{Cr}_{2p}$ atomic ratio
1Mn-n	3.9 ± 1.6	6.2	1.5	31.2
2Mn-n	9.3 ± 2.1	5.7	3.3	37.8
3Mn-n	14.3 ± 0.6	3.4	2.2	34.3
1Mn-a	1.4 ± 0.3	7.8	n.d.	4.8
2Mn-a	2.8 ± 0.5	8.1	5.1	n.d.
3Mn-a	4.3 ± 0.5	8.2	6.5	6.6

n.d.: not determined.

The results of mass loss determined during the adherence test are reported in Tab. 1 as percentage of weight loss. Weight losses for the monoliths prepared with manganese acetate were slightly higher than those for monoliths prepared with manganese nitrate.

3.2 XRD

X-ray diffractograms are displayed in Fig. 2. The bare monolith (BM: AISI 304 austenitic stainless steel treated at $900 \text{ }^\circ\text{C}$ for 2 h in synthetic air flow) presents the diffraction lines corresponding to the austenitic phase with fcc structure ($2\theta = 66.9^\circ, 79.1^\circ, 128.7^\circ$), characteristic of AISI 304 stainless steel and also the diffraction lines of martensite phase (bcc structure) at $2\theta = 68.6^\circ, 106.0^\circ$; Cr_2O_3 ($2\theta = 36.5^\circ, 50.7^\circ, 85.8^\circ$), and $\text{Mn}_{1+x}\text{Cr}_{2-x}\text{O}_{4-x}$ spinel phase ($2\theta = 45.0^\circ, 53.3^\circ, 100.2^\circ$). These assignments are in agreement with the results reported by other authors [6, 14], although they obtained the X-ray diffractograms using Cu-K α radiation.

In the diffractograms of the monolithic catalysts, besides the diffraction lines corresponding to the support, the characteristic lines of Mn_2O_3 (PDF 41-1442) were detected. As expected, the intensity of these lines increased with the impregnation numbers. Taking as reference the intensity of the diffraction lines of the austenitic phase, a notably higher intensity of the diffraction lines of Mn_2O_3 in the monoliths impregnated with manganese acetate was observed.

3.3 Surface Areas

The results of surface areas for each monolith are presented in Tab. 1. In the cases of BM and 1Mn-a, it was not possible to make the measurement with our experimental equipment, probably because the area was lower than 1 m^2 . The surface areas of the monoliths impregnated with manganese acetate (2Mn-a and 3Mn-a) are slightly higher than the monoliths impregnated with manganese nitrate.

3.4 XPS

The analysis by XPS indicated that the predominant elements on the surface were manganese and chromium. The Fe_{2p} signal was very weak and hence, iron quantification was not possible. Therefore, $\text{Mn}_{2p3/2}/\text{Cr}_{2p}$ atomic ratios were calculated in order to analyze the effect of the manganese impregnation on the surface composition. The results are indicated in Tab. 1. The Mn/Cr surface atomic ratios for the monoliths impregnated with manganese nitrate (around 34.5 ± 3.3) became considerably greater than for the monoliths impregnated with manganese acetate (around 5.7 ± 0.9). Besides, it is observed that the impregnation number did not modify significantly the Mn/Cr surface atomic ratio.

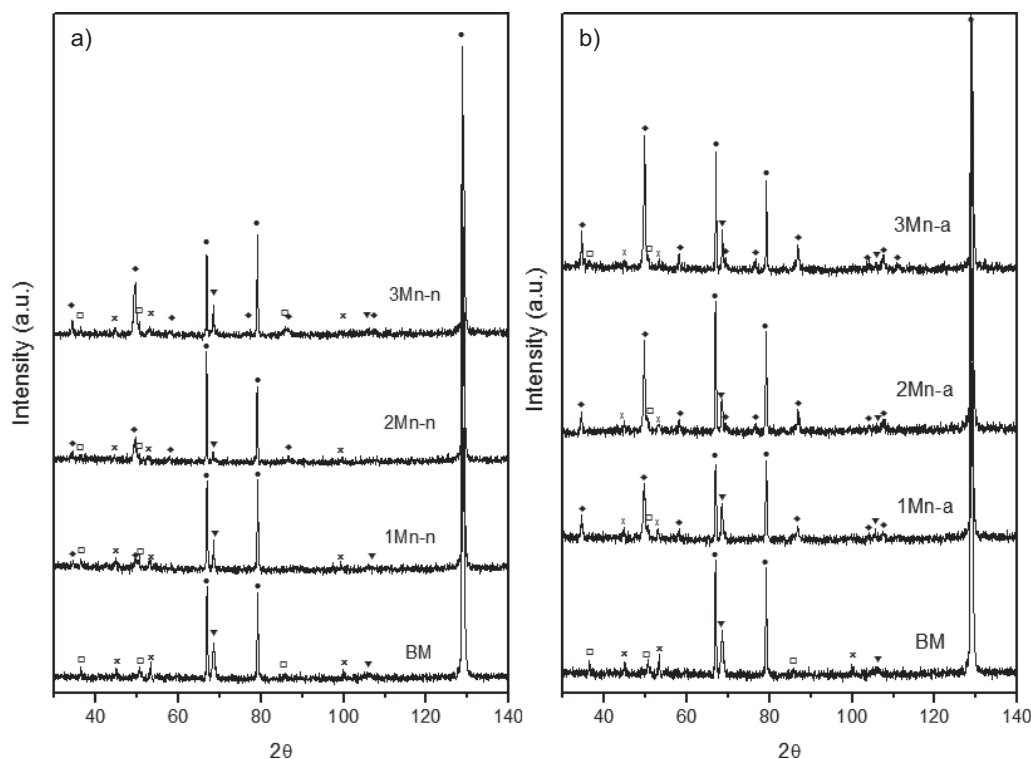


Figure 2. XRD of monoliths impregnated with (a) manganese nitrate, (b) manganese acetate. (●) Austenite, (▼) martensite, (□) Cr_2O_3 , (X) $\text{Mn}_{1+x}\text{Cr}_{2-x}\text{O}_{4-x}$, (◆) Mn_2O_3 .

3.5 Catalytic Activity

As a result of the ethyl acetate combustion reaction, total oxidation products (CO_2 and water), and intermediate products (ethanol and acetaldehyde) were detected. The curves of ethyl acetate conversion as a function of the reaction temperature are displayed in Fig. 3. The BM was active, although its activity was much lower than that of the monoliths impregnated with manganese. In general, the monoliths impregnated with manganese acetate were more active than those impregnated with manganese nitrate.

The curves of ethyl acetate conversion of 1Mn-n and 3Mn-n were practically parallel, with a $13\text{ }^\circ\text{C}$ – $23\text{ }^\circ\text{C}$ difference, with 1Mn-n being more active. At low reaction temperatures (below $220\text{ }^\circ\text{C}$, as conversion was lower than 30%), 2Mn-n was more active than 1Mn-n and 3Mn-n but at higher reaction temperatures, 2Mn-n was the least active monolith.

For the monoliths impregnated with manganese acetate, the activity increased with the impregnation number: $1\text{Mn-a} < 2\text{Mn-a} \approx 3\text{Mn-a}$. The great similarity of the last monoliths could be due to the fact that the monoliths evaluated in the catalytic test had a similar amount of active phase (173 mg in 2Mn-a and 205 mg in 3Mn-a).

Taking into account that the objective of these catalysts is the application in the total oxidation of VOCs, it is interesting to analyze the selectivity results. The curves of CO_2 yield are presented in Fig. 4. As it can be observed, the CO_2 yield became important when the conversion was higher than 80%. This clearly indicates that the reaction occurred in serial steps through the formation of intermediates, ethanol, and acetaldehyde.

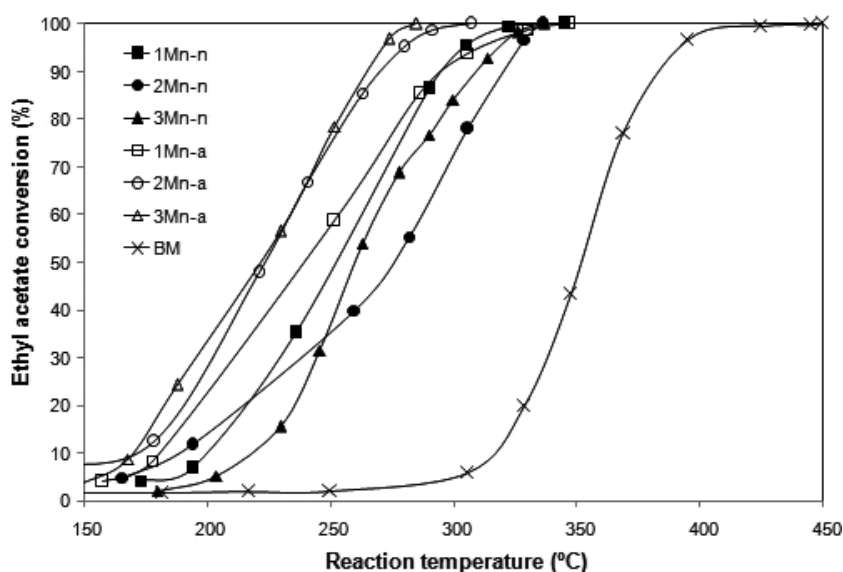


Figure 3. Curves of catalytic activity in ethyl acetate combustion.

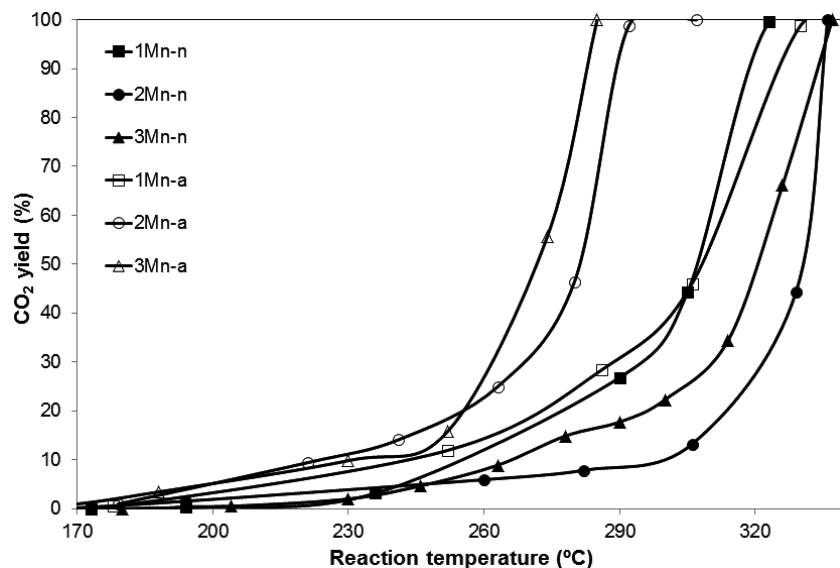


Figure 4. Curves of CO₂ yield in ethyl acetate combustion.

Selectivity curves of these intermediate compounds are presented in Fig. 5. In general, the monoliths impregnated with acetates are more selective to the production of acetaldehyde and ethanol. The order of CO₂ yield had almost the same tendency like the activity, although a slightly higher CO₂ yield on the 3Mn-a monolith was observed.

4 Discussion

It is well known that the major challenge during the preparation of metallic monolithic catalysts is to obtain a homogeneous and well-adhered active phase layer on the monolith walls. A good adherence is important to assure the durability of the catalyst operating at high space velocities of the gaseous

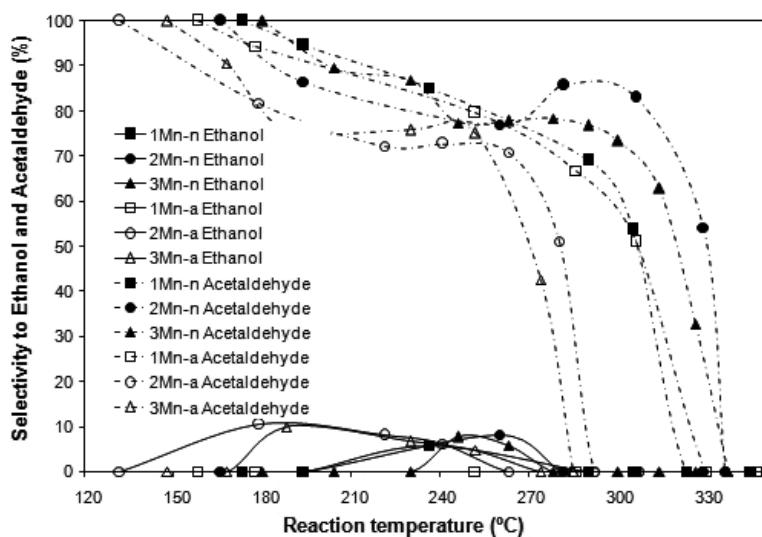


Figure 5. Curves of selectivity to ethanol and acetaldehyde.

stream, such as the conditions of combustion of VOCs. The monolith catalysts prepared in this work presented a weight loss of active phase lower than 10%. This indicates that the impregnation method generates an excellent adherence of the catalyst layer. Another great advantage of the preparation method is the high reproducibility. Numerous monoliths of each type were prepared and, as it can be observed in Fig. 1, the maximum variation of weight gain was only 2.1%.

The first important distinction by the use of different precursors is a higher weight gain achieved for the monoliths impregnated with manganese nitrate. Probably, this is due to a higher concentration of the manganese nitrate solution. Nevertheless, a different interaction between the precursors and the surface of the metallic substrate cannot be excluded. In fact, the monoliths impregnated with manganese nitrate exhibited a higher adherence than

those impregnated with manganese acetate. This could be due to a stronger interaction of the nitrate precursor with the oxide scale of the metallic surface.

Generally, there is a linear relationship between catalytic activity and the amount of active phase deposited. However, in the actual case, the monoliths impregnated with manganese acetate are more active than the monoliths impregnated with manganese nitrate, despite containing less mass of catalyst. This could be due to different dispersions of the active phase on the oxide scale when different precursors are used.

Then, with the purpose of explaining the unusual catalytic behavior, the manganese dispersion was analyzed based on the XPS results. Since iron could not be quantified, chromium was considered as a reference element of the surface oxide scale. According to Tab. 1, the Mn_{2p3/2}/Cr_{2p} surface atomic ratio for monoliths impregnated with manganese nitrate was around six-fold higher than for monoliths impregnated with manganese acetate. Even though a higher proportion of manganese in monoliths impregnated with manganese nitrate is expected because they have a higher amount of active phase, the difference of Mn/Cr atomic ratio is very significant. In fact, 1Mn-n and 3Mn-a present similar weight mass (ca. 4%), but the Mn/Cr atomic ratio of 1Mn-n is much higher than that of 3Mn-a. Hence, it is evident that the usage of manganese nitrate as precursor higher led to manganese dispersion. High dispersion of the active phase is generally a desirable characteristic in supported catalysts, but in the current case, this did not generate a better catalytic behavior. This anomalous result supports the conclusion that each precursor generates unlike phases on the surface.

By means of XRD, only the formation of crystalline Mn₂O₃ can be identified (Fig. 2). However, it is worth mentioning that the diffraction lines of

Mn_2O_3 in samples impregnated with manganese acetate are more intense than in samples impregnated with manganese nitrate, despite the differences of weight gain during impregnation. Then, it is deduced that not all manganese deposited from manganese nitrate forms crystalline Mn_2O_3 . A possible explanation is the formation of amorphous MnO_x species highly dispersed on the surface which are undetectable by XRD, such as those obtained on alumina [13]. The XPS results support this conclusion but dispersed surface MnO_x species are recognized as highly active species in catalytic oxidation and this is not observed in our catalysts impregnated with manganese nitrate. Consequently, this elucidation is rather unlikely. Another possibility is that the manganese incorporated by impregnation reacted with the oxides of the scale forming a less active phase than Mn_2O_3 .

The reaction between the manganese impregnated from manganese nitrate and the oxides formed on the steel surface could be favored by the acid pH of the manganese nitrate solution (pH 2). At this pH, part of the Cr_2O_3 exposed on the steel surface can be dissolved and thus, some chromium would be co-impregnated with manganese. After drying and calcination at 500°C , the formation of an Mn-Cr-O mixed phase is highly feasible. Also, it is not rejected that the oxidizing character of NO_3^- ions could cause the oxidation of Cr^{3+} species to Cr^{6+} , resulting in the formation of CrO_4^{2-} in the solution [15] and leading to the formation of manganese chromate on the surface after calcination.

The major adherence of the active phase in the monoliths impregnated with manganese nitrate with regard to those impregnated with manganese acetate supports the idea of a strong interaction between the deposited phase and the oxides of the passive scale as result of a chemical reaction. The high Mn/Cr surface atomic ratio determined by XPS for the monoliths impregnated with manganese nitrate suggests a high dispersion of the Mn-Cr-O mixed phases. The results of surface area are in line with this perception. The monoliths impregnated with manganese nitrate present lower surface areas than those impregnated with manganese acetate. This could be explained assuming that the phases formed from manganese nitrate covers the surface of the bare monolith, whereas the poorly dispersed Mn_2O_3 phase in monoliths impregnated with manganese acetate segregates, increasing the surface area of the monoliths. The small increase of surface area observed in the monoliths impregnated with manganese acetate could be the cause of the highest catalytic activity. Nevertheless, the effect of the different catalyst characteristics (active phase charge, active phase nature, surface composition) resulting of the use of different manganese precursors cannot be excluded.

A schematic representation of the catalyst nature, such as it is imagined on the basis of the characterization results, is presented in Fig. 6. Impregnation with manganese nitrate covers the surface, generating a manganese-rich layer (according to XPS results) with minimal increase of surface area. Considering the XRD results, one part of manganese forms Mn_2O_3 and another part could give Mn-Cr-O mixed oxides. In contrast, the impregnation with manganese acetate results in the formation of segregated Mn_2O_3 (according to XRD results) causing a small increase of the surface area.

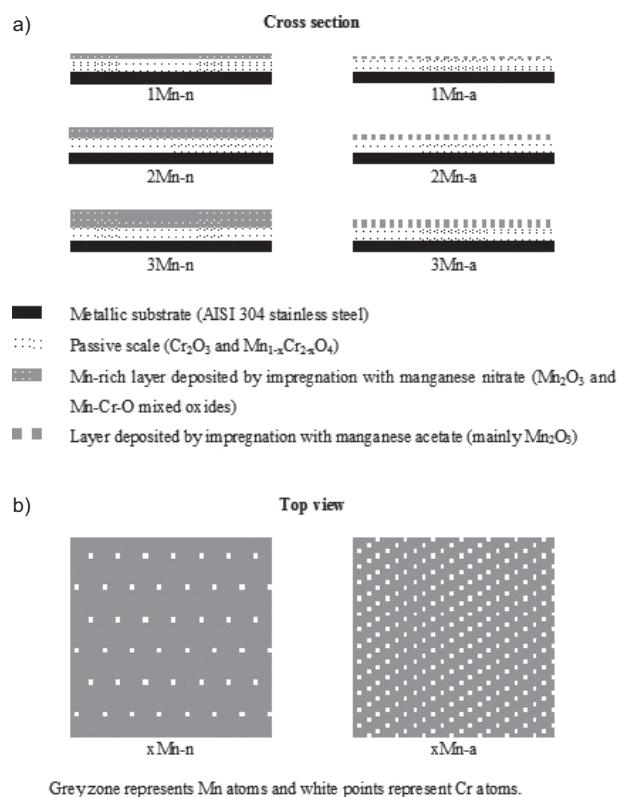


Figure 6. Representative scheme of catalysts.

5 Conclusions

The following conclusions can be inferred from the described results:

- It is possible to obtain manganese oxide-based catalysts on AISI 304 austenitic stainless-steel metallic monoliths by means of impregnation with an aqueous solution of precursor salts. This method is highly reproducible and generates a well-adhered catalytic layer.
- The application of various precursors (manganese acetate or manganese nitrate) leads to significantly different results. With manganese acetate, Mn_2O_3 with low dispersion on the surface is mainly obtained, while with manganese nitrate, the formation of Mn-Cr-O mixed phases is favored. These mixed phases ($\text{Mn}_{1+x}\text{Cr}_{2-x}\text{O}_{4-x}$ spinel and/or manganese chromate) are highly dispersed but are less active than Mn_2O_3 in the combustion of ethyl acetate.
- The best catalytic performance is achieved with monoliths impregnated with manganese acetate, being the most active and selective one that contains the highest amount of active phase.

Acknowledgment

The authors gratefully acknowledge the financial support received from UNSL, CONICET, and ANPCyT. They are also grateful to ANPCyT for the purchase of the UHV Multi Analysis System (PME 8-2003).

The authors have declared no conflict of interest.

References

- [1] K. Everaert, J. Baeyens, *Hazard. Mater.* **2004**, *109*, 113–139. DOI: 10.1016/j.jhazmat.2004.03.019
- [2] P. Avila, M. Montes, E. E. Miró, *Chem. Eng. J.* **2005**, *109*, 11–36. DOI: 10.1016/j.cej.2005.02.025
- [3] N. Burgos, M. Paulis, M. Montes, *J. Mater. Chem.* **2003**, *13*, 1458–1467. DOI: 10.1039/B212242A
- [4] B. P. Barbero, L. Costa-Almeida, O. Sanz, M. R. Morales, L. E. Cadús, M. Montes, *Chem. Eng. J.* **2008**, *139*, 430–435. DOI: 10.1016/j.cej.2007.12.03
- [5] A. Cyulski, J. A. Moulijn, *Catal. Rev. Sci. Eng.* **1994**, *36*, 179–270. DOI: 10.1080/01614949408013925
- [6] L. M. Martínez, O. Sanz, M. I. Domínguez, M. A. Centeno, J. A. Odriozola, *Chem. Eng. J.* **2009**, *148*, 191–200. DOI: 10.1016/j.cej.2008.12.030
- [7] A. M. Huntz, A. Reckmann, C. Haut, C. Sévéc, M. Herbst, F. C. T. Resende, A. C. S. Sabioni, *Mater. Sci. Eng. A* **2007**, *447*, 266–276. DOI: 10.1016/j.msea.2006.10.022
- [8] F. G. Durán, B. P. Barbero, L. E. Cadús, *Catal. Lett.* **2011**, *141*, 1786–1795. DOI: 10.1007/s10562-011-0716-x
- [9] X. Han, R. Zhou, G. Lai, X. Zheng, *Catal. Today* **2004**, *93–95*, 433–437. DOI: 10.1016/j.cattod.2004.06.053
- [10] A. C. C. Rodrigues, *Catal. Commun.* **2007**, *8* (8), 1227–1231. DOI: 10.1016/j.catcom.2006.11.013
- [11] Z. Chen, Q. Yang, H. Li, X. Li, L. Wang, S. C. Tsang, *J. Catal.* **2010**, *276* (1), 56–65. DOI: 10.1016/j.jcat.2010.08.016
- [12] D. Frías, S. Nousir, I. Barrio, M. Montes, L. M. Martínez, M. A. Centeno, J. A. Odriozola, *Appl. Catal., A* **2007**, *325* (2), 205–212. DOI: 10.1016/j.apcata.2007.02.038
- [13] F. N. Agüero, A. Scian, B. P. Barbero, L. E. Cadús, *Catal. Today* **2008**, *133–135*, 493–501. DOI: 10.1016/j.cattod.2007.11.044
- [14] L. M. Martínez, D. M. Frías, M. A. Centeno, A. Paúl, M. Montes, J. A. Odriozola, *Chem. Eng. J.* **2008**, *136*, 390–397. DOI: 10.1016/j.cej.2007.05.040
- [15] M. J. Capitan, S. Lefebvre, A. Traverse, A. Paúl, J. A. Odriozola, *J. Mater. Chem.* **1998**, *8* (10), 2293–2298. DOI: 10.1039/A802233J